AB INITIO CALCULATIONS OF STRONGLY CORRELATED ELECTRONS: ANTIFERROMAGNETIC GROUND STATE OF UO_2

YOUNSUK YUN[1], HANCHUL KIM[2], HEEMOON KIM[3] and KWANGHEON PARK[1*]
[1] Kyung-Hee University
Sochen-ri, Giheung-eup, Yongin-si, Gyeonggi-do, Korea, 440-701
[2] Korea Research Instiute of Standard and Science
P.O.Box 102, Yuseong, Daejeon, Korea
[3] Korea Atomic Energy Research Institute
150 Deokjin-dong, Yuseong-gu, Daejeon, Korea, 305-353
*Corresponding author. E-mail : kpark@khu.ac.kr

Received November 15, 2004
Accepted for Publication April 25, 2005

We have performed the density functional theory calculations of UO_2 using the spin-polarized generalized gradient approximation (SP-GGA) and the SP-GGA+U approach. The SP-GGA+U approach correctly predicts the insulating electronic structure with antiferromagnetic ordering, but the SP-GGA calculations predict metallic behavior. The cohesive properties obtained from the SP-GGA+U calculations are in good agreement with the available experimental results and previous calculations. The spin-polarized local density of states shows that the antiferromagnetic ordering of UO_2 is governed by 5f orbitals of uranium ion. Our calculations demonstrate that the strong correlation of U 5f electrons should be taken into account for a reliable description of UO_2 physics.

KEYWORDS : SP-GGA+U, Spin-polarized Local Density of States, Strong Correlation of U 5f Orbitals

1. INTRODUCTION

Uranium dioxide (UO_2) is an important fuel material in the nuclear industry, and the behavior of the 5f electrons of uranium is one of the most interesting subjects about actinide elements and their compounds. Uranium dioxide is known to be a good insulator[1], and it is also known that the magnetic moment on uranium ions orders antiferromagnetically at temperatures below 30K.[2, 3], The structural and electronic properties of UO_2 have been studied by using X-ray photoelectron spectroscopy (XPS) and Bremsstrahlung isochromat spectroscopy (BIS).[4, 5, 6] Theoretically, Kelly and Brooks[7] have performed density functional theory (DFT)[8, 9] calculations using the linear muffin-tin orbital (LMTO) method and the local density approximation (LDA)[10] to study the energy band structure of UO_2. They found that the LDA calculations fail to describe UO_2, predicting metallic behavior contrary to the observed insulating behavior. Petit *et al.* calculated the density of states and the cohesive properties of UO_2 using the LMTO method in the atomic sphere approximation (ASA).[11] They obtained a smaller lattice constant, a smaller cohesive energy, and a larger bulk modulus than the experimental values. They also observed that the ground state of UO_2 was still metallic.

The failure of the conventional DFT has been attributed to the strong correlation of 5f electrons in UO_2. Recently, theoretical calculations have been made that take into account this strong correlation. For instance, Dudarev *et al.*[12] obtained the correct insulating ground state of UO_2 from the local spin density approximation (LSDA)+U calculations that were proposed by Anisimov *et al.*[13] In addition, Kudin *et al.* compared the results from DFT calculations using LSDA, a generalized gradient approximation (GGA),[14] and a hybrid DFT functional. They demonstrated that the hybrid DFT method successfully describes the electronic and the magnetic structure of UO_2.[15] Very recently, Laskowski *et al.* investigated the magnetic structure of UO_2 using the linear augmented plane wave method with spin-orbit coupling.[16] They compared different LDA+U schemes by calculating the uranium electric field gradients.

In this work, we report on a comparative study of the conventional spin-polarized GGA (SP-GGA) and the SP-GGA+U calculations for UO_2. The ground state of UO_2 was found to be insulating when the electronic correlation

is properly described. In addition, the ground state shows an antiferromagnetic ordering of magnetic moments localized at U ions. The structural and the thermodynamic parameters were determined from the calculated equation of states, and these parameters agreed well with available experimental results. The angular-momentum-decomposed local density of states (LDOS) reveals that the introduction of U properly describes both the strong correlation of U $5f$ orbitals and the hybridization between the U $5f$ and O $2p$ orbitals. The spin-decomposed LDOS reveals that the antiferromagnetic ordering of UO_2 is due to two unpaired $5f$ electrons. In section II, we briefly describe the GGA+U formalism based on DFT. In section III, we present our results and discuss them. Finally, we provide our conclusion in section IV.

2. METHODOLOGY

The density functional theory is a quantum mechanical approach to predicting the ground-state properties of materials, it has been successfully applied to such things as bulk materials, surfaces, interfaces, superlattices, and point defects. The most prominent feature of DFT, as compared with previous many-body theories, is that it describes the interacting electrons by means of the single -electron density without introducing approximate many-body wave functions. In 1964, Hohenberg and Kohn[8] proved that the total energy of an electron gas is a unique functional of the single-electron density. The electron density minimizing the total energy functional is the exact single-particle density of the ground state. Subsequently, Kohn and Sham[9] have provided a practical scheme, in which the total-energy functional is expressed, using a set of fictitious single-particle orbitals, ψ_i, as follows:

$$E[\{\psi_i\}] = \sum_i \int \psi_i^* \left(-\frac{\hbar^2}{2m}\right) \nabla^2 \psi_i d^3\vec{r} + \int V_{ion}(\vec{r}) n(\vec{r}) d^3\vec{r} + \frac{e^2}{2} \iint \frac{n(\vec{r}) n(\vec{r}')}{|r - r'|} d^3\vec{r} d^3\vec{r}' + E_{XC}[n(\vec{r})] + E_{ion}(\{\vec{R}_I\}) . \quad (1)$$

In Equation 1, E_{ion} is the Coulomb energy associated with interactions among the nuclei at positions $\{\vec{R}_i\}$, V_{ion} is the electron-ion potential, $n(\vec{r})$ is the electronic density given by

$$n(\vec{r}) = \sum_i^{occupied} |\psi_i(\vec{r})|^2 , \quad (2)$$

and $E_{XC}[n(\vec{r})]$ is the exchange-correlation energy functional. For a given ionic configuration, $\{\vec{R}_i\}$, the minimum value of the Kohn-Sham energy functional is equal to the total energy of the electronic ground state. Therefore, it is necessary to determine the set of wave functions, ψ_i, that minimizes the Kohn-Sham energy functional. This can be done by numerically obtaining the solution to the Schrödinger-like equations of materials, the so-called Kohn-Sham equations,

$$\left[\frac{-\hbar^2}{2m}\nabla^2 + V_{ion}(\vec{r}) + V_H(\vec{r}) + V_{XC}(\vec{r})\right]\psi_i(\vec{r}) = \varepsilon_i \psi_i(\vec{r}) , \quad (3)$$

where ψ_i is the wave function of electronic state i, ε_i is the corresponding Kohn-Sham eigenvalue, and the terms inside the square bracket can be regarded as an effective single-particle Hamiltonian. The Hartree potential of the electrons, V_H, is given by

$$V_H = e^2 \int \frac{n(\vec{r}')}{|\vec{r} - \vec{r}'|} d^3\vec{r}' . \quad (4)$$

The exchange-correlation potential, V_{XC}, is given formally by the functional derivative

$$V_{XC} = \frac{\delta E_{XC}[n(\vec{r})]}{\delta n(\vec{r})} . \quad (5)$$

The Kohn-Sham equations represent a mapping of the interacting many-electrons system onto a system of non-interacting electrons under an effective potential caused by the other electrons. The Kohn-Sham equations must be solved self-consistently: the occupied electronic states generate a charge density that produces the electronic potential that is used to construct the equation.

As stated above, the exchange-correlation contribution in Eq. (3) is only a formal expression. The simplest and most common approach for the practical implementation of the exchange-correlation interaction is the LDA. In the LDA, E_{XC} is constructed by assuming that the exchange-correlation energy per electron at a point $\vec{r}$ in the electron gas, $\varepsilon_{XC}(\vec{r})$, is equal to the exchange-correlation energy per electron in a homogeneous electron gas that has the same density as the electron gas at point $\vec{r}$.

$$E_{XC}[n(\vec{r})] = \int \varepsilon_{XC}(\vec{r}) n(\vec{r}) d^3\vec{r} \quad (6)$$

From its construction, the LDA has problems in describing systems with rapidly varying charge density. Thus, the GGA incorporates the effect of spatially varying the charge density by adding dependence on the charge density gradient of Eq. (6). Nevertheless, both the LDA and the GGA are known to have difficulty describing the electronic structure of the strongly correlated materials. The $5f$ orbital in the actinide atoms and compounds is one example of the strong Coulomb repulsion effects. Researchers have proposed different remedies to compensate for the incapability of the LDA. For instance, Anisimov *et al.*[17,18] proposed a simplified version of the LSDA+U energy functional, however, their version is not invariant with respect to

unitary transformation. Later, Dudarev *et al.* [23] corrected the functional of Anisimov *et al.* into the covariant form shown below,

$$E_{LSDA+U} = E_{LSDA} + \frac{1}{2}(\bar{U} - \bar{J})\sum_{\sigma}(\mathrm{Tr}\,\rho^{\sigma} - \mathrm{Tr}(\rho^{\sigma}\rho^{\sigma})) \quad (7)$$

where ρ is the density matrix of f electrons, σ is the projection of spin, and $\bar{U}$ and $\bar{J}$ are the spherically averaged matrix elements of screened Coulomb electron-electron interaction. This approach can be interpreted as the addition of a penalty functional to the conventional DFT-LDA total energy, which forces the on-site Coulomb repulsion. It is important to note that the total energy will depend on the parameters $\bar{U}$ and $\bar{J}$. As seen in Eq. (7), the parameters $\bar{U}$ and $\bar{J}$ do not enter separately and the difference ($\bar{U}$-$\bar{J}$) is only meaningful.

In this work, we performed the SP-GGA and the SP-GGA+U calculations using the Perdew-Wang 91[14] exchange-correlation functional and a plane-wave basis, as implemented in the Vienna *Ab initio* Simulation Package (VASP).[19, 20] We used the Dudarev's simplified scheme to include the Coulomb correlation U. The electron-ion interaction was described by the projector-augmented-wave (PAW) potential.[21, 22] Within the PAW scheme, the wave functions are expanded by (i) the plane waves and (ii) the atomic and pseudo-atomic orbitals centered at each atom. The plane wave part has the flexibility to describe the bonding and interstitial region, but it would require a prohibitively large basis set to describe correctly the nodal structure of the wave the function near the nucleus. Thus, the atomic orbitals were introduced to represent the core region. Plane waves with a kinetic energy of up to 400 eV were used to expand the wave functions. The charge density was obtained by using 6 × 6 × 4 k-point grid within the Brillouin zone. The Wigner-Seitz radii of U and O atoms were chosen to be 1.42 and 0.73 Å, respectively. The parameters for the SP-GGA+U were taken to be $\bar{U}$ = 4.5 eV and $\bar{J}$ = 0.5 eV, following Dudarev *et al.*[12,17,18] We note that the 5f Coulomb correlation energy was determined to be 4.6 ± 0.8 eV from the energy difference in the two spectroscopy experiments (XPS and BIS)[1].

3. RESULTS AND DISCUSSION

The paramagnetic phase of UO_2 belongs to the cubic space group F_{m3m}. In the ground state, uranium dioxide exhibits antiferromagnetism, and the magnetic moments at U ions are antiferromagnetically ordered in the [001] direction, as illustrated in Fig. 1(a).[2,3] Figure 1(b) shows the tetragonal unit cell used in this work.

First, we calculated the total energy of UO_2 by varying the lattice constants to determine the theoretical lattice constant. The calculated equilibrium lattice constant was 5.44 Å that is underestimated by about 0.6 % compared with the experimental value of 5.46 Å. The results are fitted to Birch's equation of state and are plotted in Fig. 2. In Table 1, the calculated values of the structural, thermodynamic, electronic, and magnetic properties of UO_2 are compared with experimental results [1,4,5,6,19,20] and previous calculations[11,12,23,24] The cohesive energy was calculated to be 20.26 eV/UO_2, which was estimated by subtracting the fully spin-polarized atomic total energies of U and O from the total energy of UO_2. This calculation was smaller than the experimental value of 22.31eV by about 9 %.

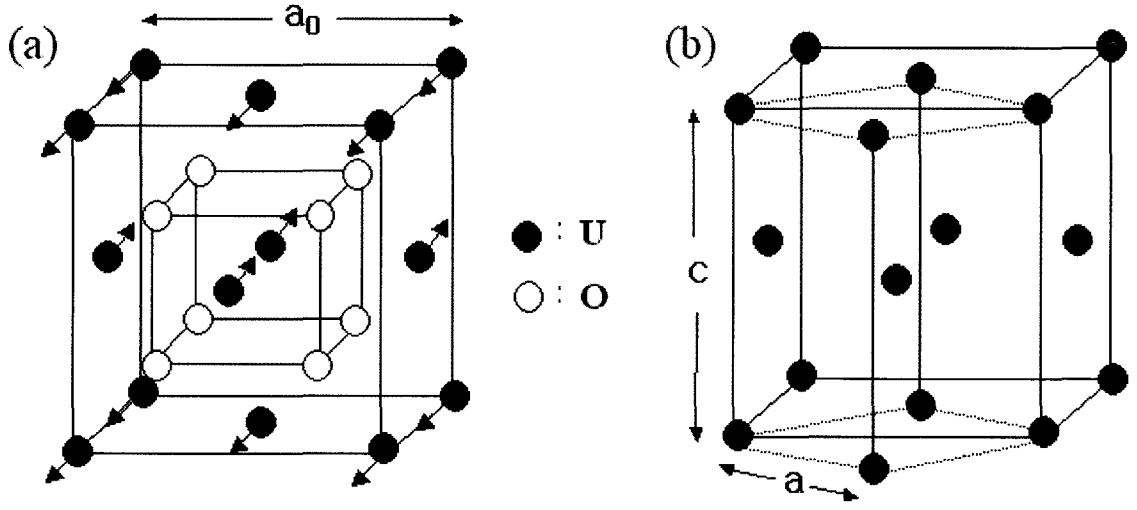

Fig. 1. The Structure of Bulk UO_2: (a) a Conventional Unit Cell Showing Antiferromagnetic Ordering of Spins in the [001] Direction and (b) a Tetragonal Primitive Unit Cell of the Antiferromagnetic Phase.[14] The a_0 Indicates the Lattice Constant of UO_2. The c is Equal to a_0 and the c/a Ratio is $\sqrt{2}$

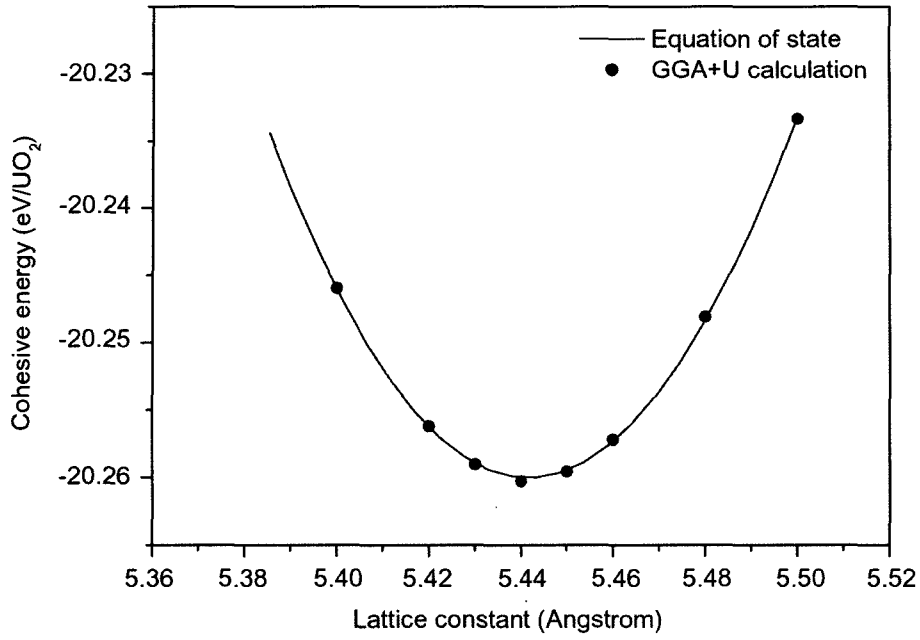

Fig. 2. The Equation of State of UO_2 Shows the Dependence of Total Energy on the Lattice Constant. The Calculated Results are Indicated by Solid Circles and the Fit to Birch's Formula is Plotted by a Solid Line

Table 1. The Calculated Properties of UO_2 Obtained from GGA+*U* Calculations are Compared with Experimental Results and Previous Theoretical Calculations

	Experiment[a]	T. Petit[b] (LMTO-LDA)	S.L. Dudarev[c] (LMTO-LSDA+*U*)	This work (PAW-GGA+*U*)
Lattice constant (Å)	5.46	5.25	5.37	5.44
Cohesive energy (eV/ UO_2)	22.31	18.63	22.23	20.26
Bulk modulus (GPa)	207	252	202	209
Magnetic moment of U (μ_B)	1.74	-	1.70	1.89*
Band gap (eV)	2.0	-	2.1	1.8

[a]Ref. 1, 4, 5, 6, 25, 26. [b]Ref. 11. [c]Ref. 12, 23, 24.
*This estimate for the magnetic moment was obtained by subtracting the integrated density of spin-down electrons from that of spin-up electrons within a spherical volume of radius 1.42Å.

Figure 3 shows the local density of states (LDOS) of UO_2 obtained from both the SP-GGA and SP-GGA+*U* calculations. The SP-GGA+*U* calculations predict the correct insulating ground state with an energy band gap of 1.8 eV. In contrast, calculations employing the original SP-GGA result in a metallic electronic structure, where the U 5*f* bands are partially occupied. This clearly demonstrates that the insulating nature of the ground state results from the presence of the strong correlation among U 5*f* electrons. The band gap is opened up, due to the split 5*f* bands, and agrees well with the experimental value of 2.0 eV. In both the SP-GGA and SP-GGA+*U* approaches, the conduction bands are mainly derived from U 5*f* and 6*d* orbitals, and the valence bands are mainly derived from O 2*p* and U 5*f* orbitals. It is known that U 5*f* and O 2*p* orbitals form covalent bonds in UO_2.[27, 28] In the right panel of Fig. 3, the coincident peak structure is prominent in the U 5*f* LDOS and in the O 2*p* LDOS just below the Fermi level, and this seems to indicate hybridization between the U 5*f* and O 2*p* orbitals. This phenomenon feature is negligible in the SP-GGA case (see the left panel of Fig. 3), which suggests that the hybridization between the U and O ions is better described when including the on-site Coulomb correlation, *U*. The spin and angular-momentum decomposed LDOS of a U ion is shown in Fig. 4. The spin-down component of the U 5*f* shell is almost completely

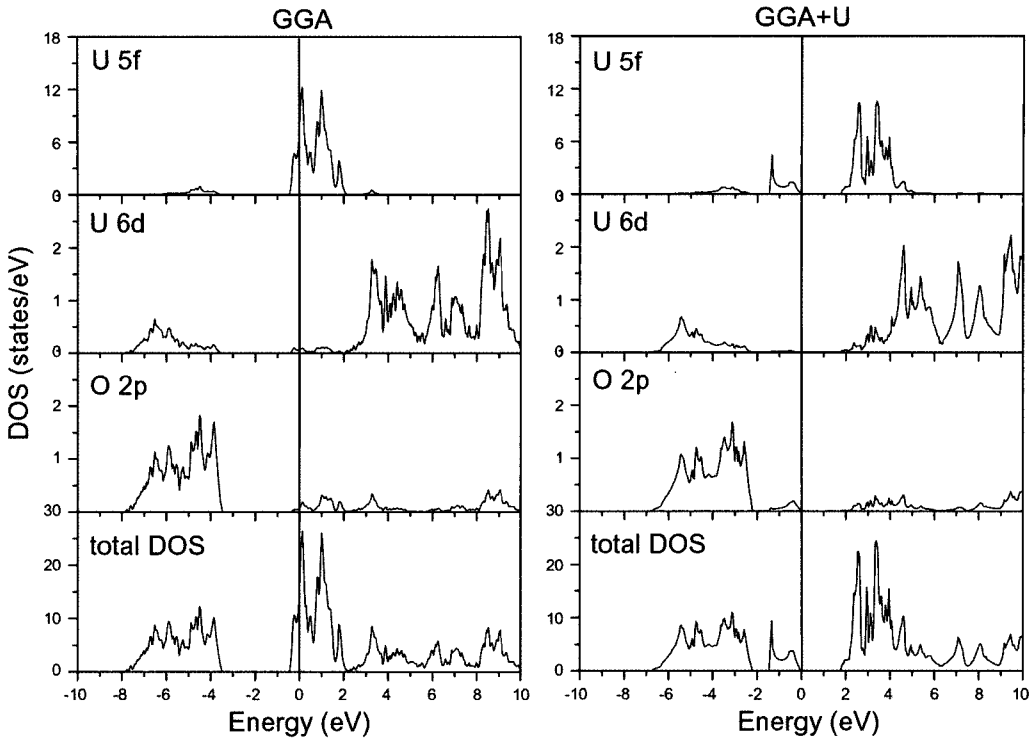

Fig. 3. The Local Density of States Projected to the U 5f and 6d Orbitals and to the O 2p State for the AntiferromagneticUO_2: (left) GGA Results and (right) GGA+U Results. Notice that, Contrary to the GGA Result Predicting Metallic Behavior, a Band Gap of 1.8 eV is Opened Up in the GGA+U Case. The Energy is Referred to the Fermi Level

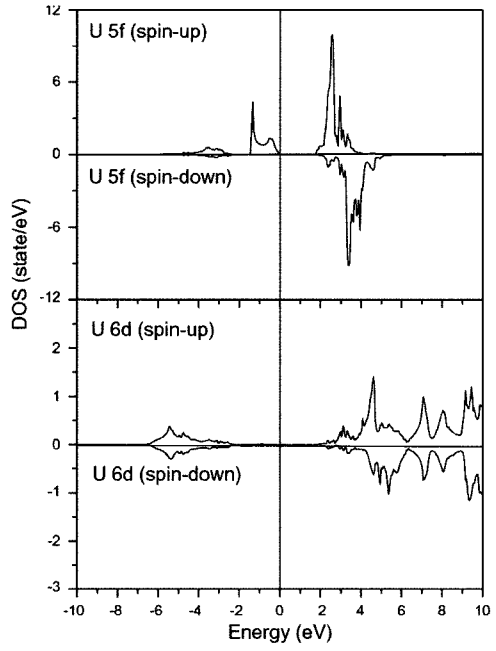

Fig. 4. The Spin-decomposed and Symmetry-resolved Local Density of States for U 5*f* and 6*d* Orbitals. The Difference in the Spin-up and Spin-down DOS of U 5*f* State Leads to the Antiferromagnetic Ordering of UO_2. Birch's Formula is Plotted by a Solid Line

unoccupied, and thus a non-zero magnetic moment is developed at each U ion. Those localized moments point in alternating opposite directions along the [001] direction, as illustrated in Fig. 1(a), to constitute the antiferromagnetic ordering. The spin-polarization in the U 6*d* shell is found to be significantly smaller than that in the 5*f* shell. The magnetizations of 6*d* and 5*f* shells at two inequivalent U atoms in the unit cell (see Fig. 1) are $\pm 0.02\ \mu_B$ and $\pm 1.85\ \mu B$, respectively, and the total magnetic moment of each U ion is $\pm 1.89\ \mu_B$. These results suggest that the magnetic structure of UO_2, i.e., the antiferromagnetism in the ground state, is governed by the almost complete spin-polarization of the partially filled U 5*f* bands.

4. CONCLUSIONS

We investigated the structural, thermodynamic, electronic, and magnetic properties of UO_2, using the DFT calculations within the SP-GGA+*U* scheme and the PAW potentials. The insulating behavior of UO_2 was well reproduced, as evidenced by the calculated band gap opening, and our other calculated results are in good agreement with the experimented data. From the spin-decomposed LDOS of UO_2, we found that U 5*f* orbitals

are split into two lumps, and the energy gap occurs between the two lumps. The spin-decomposed LDOS suggests that the magnetism of UO_2 is stabilized by a correlation among the partly filled 5f orbitals. The U 5*f* orbitals also actively participate in forming covalent bonds with neighboring O 2*p* orbitals. The hybridization between the occupied U 5*f* bands and the top of the O 2*p* valence bands around the gap manifests itself more clearly in the GGA+*U* calculation than it does in the GGA calculation.

REFERENCES

[1] Y. Baer and J. Schoenes, "Electronic Structure and Coulomb Correlation Energy in UO_2 Single Crystal", *Solid State Commun.* **33**, 885 (1980).

[2] L. Lynds, "Preparation of Stoichiometric UO_2 by Thermal Decomposition of UO_2I_2", *J. Inorg. Nucl. Chem.* **24**, 1007 (1962).

[3] A.P. Cracknell and M.R. Daniel, "Magnetic Point Groups Selection Rules and Antiferromagnetic Phase Transition in UO_2", *Proc. Phys. Soc.* **92**, 705 (1967).

[4] B. W. Veal, and D. J. Lam, "X-ray Photoelectron Studies of Thorium, Uranium, and Their Dioxides", *Phys. Rev.* B **10**, 4902 (1974).

[5] J. Verbist, J. Riga, J. J. Pireaux, and R. Caudano, "X-ray Photoelectron spectra of uranium and uranium oxides. Correlation with the half-life of $^{235}U^{m}$", *J. Electron Spectrosc. Relat. Phenom.* **5**, 193 (1974).

[6] L. E. Cox, "XPS evidence for 5f bonding participation in UO_2", *J. Electron Spectrosc. Relat. Phenom.* **26**, 167 (1982).

[7] P. J. Kelly and M. S. S. Brooks, "Electronic Structure and Ground –state Properties of the Actinide Dioxide", *J. Chem. Soc. Faraday Trans.* II, **83**, 1189 (1987).

[8] P. Hohenberg and W. Kohn, "Inhomogeneous Electron Gas", *Phys. Rev*, **136**, B664 (1964).

[9] W. Kohn and L. J. Sham, "Self-Consistent Equations Including Exchange and Correlation Effects", *Phys. Rev.* **140**, B1133 (1965).

[10] D. M. Ceperley and B. J. Alder, "Ground State of Electron Gas by a Stochastic Method", *Phys. Rev. Lett.* **45**, 566 (1980).

[11] T. Petit *et al.*, "Cohesive Properties of UO_2", *Phil. Mag.* B **73**, 893 (1996).

[12] S. L. Dudarev, D. Nguyen Manh, and A. P. Sutton, "Effect of Mott-Hubbard correlations on the Electronic Structural Stability of Uranium Dioxide", Phil. Mag. B **75**, 613 (1997).

[13] V.I. Anisimov, J. Zaanen, and O. K. Andersen, "Band Theory and Mott Insulators: Hubbard *U* instead of Stoner *I*", *Phys. Rev.* B **44**, 943 (1991).

[14] J. P. Perdew and Y. Wang, "Accurate and Simple analytic Representation of the Electron-Gas Correlation Energy", *Phys. Rev.* B **45**, 13244 (1992).

[15] K. N. Kudin *et al.*, "Hibrid Density-Functional Theory and the Insulating Gap of UO_2", *Phys. Rev. Lett.* **89**, 266402 (2002).

[16] R. Laskowski, G. K. H. Madsen, P. Blaha, and K. Schwarz, "Magnetic Structure and Electronic-Field Gradients of Uranium Dioxide: An ab initio study", *Phys. Rev.* B **69**, 140408(R) (2004).

[17] I.V. Solovyev, P.H. Dederichs, and V.I. Anisimov, "Corrected Atomic Limit in the Local-Density Approximation and the Electronic Structure of d impurities in Rb", *Phys. Rev.* B **50**, 16861 (1994).

[18] A.I. Liechtenstein, V.I. Anisimov, and J. Zaanen, "Density -Functional Theory and Strong Interactions: Orbital ordering in Mott-Hubbard Insulator", *Phys. Rev.* B **52**, R5467 (1995).

[19] G. Kresse and J. Hafner, "*Ab Initio* Molecular Dynamics for Liquid Metals", *Phys. Rev.* B **47**, RC558 (1993).

[20] G. Kresse and J. Furthmüller, "Efficient Iterative Schemes for Ab initio Total-Energy Calculations Using a Plane-Wave Bases Set", *Phys. Rev.* B **54**, 11169 (1996).

[21] P.E. Blöchl, "Projector Augmented-Wave Method", *Phys. Rev.* B **50**, 17953 (1994).

[22] G. Kresse and J. Joubert, "From Ultrasoft Pseudopotentials to the Projector Augmented-Wave Method", *Phys. Rev.* B **59**, 1758 (1999).

[23] S.L. Dudarev, G.A. Botton, S.Y. Savrasov, C.J. Humphreys, and A.P. Sutton, "Electron-Energy-Loss Spectra and the Structural Stability of Nickel Oxide: An LSDA+U Study", *Phys. Rev.* B **57**, 1505 (1998).

[24] S.L. Dudarev, G.A. Botton, S.Y. Savrasov, Z. Szotek, W. M. Temmerman, and A.P. Sutton, "Elctronic Structure and Elastic Properties of Strongly Correlated Metal Oxides form First Principles : LSDA+U, SIC-LSDA and EEES Study of UO_2 and NiO", *Phys. Stat. Sol.* **166**, 429 (1998).

[25] D. G. Martin, *High Temp.-High Pressures* **21**, 13 (1989).

[26] Landolt-Börnstein, "Magnetic and other properties of oxides and related compounds. Part C Hexagonal ferrites, special lanthanide and actinide compounds", Ed. K.-H. Hellwege and A.M. Hellwege, **Vol. 12**, Numerical Data and Functional Relationships in Science and Technology. New series. Group III: Crystal and Solid State Physics., *Springer-Verlag*, Berlin (1982).

[27] S. Xia and J.C. Krupa, "Calculated variation trends across the actinide dioxide series: electronic structure and charge transfer transitions", *J. Alloys Compd.* **307**, 61 (2000).

[28] C. Gunnarsson, D. D. Sarma, F. U. Hillebrecht, and K. Schönhammer, "Electronic structure of the light actinide oxides from electron spectroscopy", *J. Appl. Chem.* 63, 3676 (1988).